Received: 7 July 2023 | Revised: 15 September 2023 | Accepted: 17 October 2023

DOI: 10.1002/jemt.24448

RESEARCH ARTICLE

MICROSCOPY RESEARCH & TECHNIQUE WILEY

Preparation of atom probe tips from (nano)particles in dispersion using (di)electrophoresis and electroplating

Nora Vorlaufer[1] | Jan Josten[1] | Simon Carl[2] | Erik Göbel[1] | Alexander Søgaard[3,4] | Nicola Taccardi[3] | Erdmann Spiecker[2] | Peter Felfer[1]

[1]Institute I, Materials Science & Engineering Department, Friedrich-Alexander-Universität Erlangen-Nürnberg, Erlangen, Germany

[2]Institute of Micro- and Nanostructure Research (IMN) and Center for Nanoanalysis and Electron Microscopy (CENEM), Materials Science & Engineering Department, Friedrich-Alexander-Universität Erlangen-Nürnberg, Erlangen, Germany

[3]Institute of Chemical Reaction Engineering, Department Chemical and Biological Engineering, Friedrich-Alexander-Universität Erlangen-Nürnberg, Erlangen, Germany

[4]CHEC Research Centre, Department of Chemical and Biochemical Engineering, Technical University of Denmark, Kongens Lyngby, Denmark

Correspondence
Nora Vorlaufer, Institute I, Materials Science & Engineering Department, Friedrich-Alexander-Universität Erlangen-Nürnberg, Erlangen, Germany.
Email: nora.vorlaufer@fau.de

Funding information
Deutsche Forschungsgemeinschaft

Review Editor: Paul Verkade

Abstract

The behavior of catalytic particles depends on their chemical structure and morphology. To reveal this information, the characterization with atom probe tomography has huge potential. Despite progresses and papers proposing various approaches towards the incorporation of particles inside atom probe tips, no single approach has been broadly applicable to date. In this paper, we introduce a workflow that allowed us to prepare atom probe specimens from Ga particles in suspension in the size range of 50 nm up to 2 µm. By combining dielectrophoresis and electrodeposition in a suitable way, we achieve a near-tip shape geometry, without a time-consuming FIB lift-out. This workflow is a simple and quick method to prepare atom probe tips and allows for a high preparation throughput. Also, not using a lift-out allowed us to use a cryo-stage, avoiding melting of the Ga particles, while ensuring a mechanical stable atom probe tip. The specimen prepared by this workflow enable a stable measurement and low fracture rates.

Research Highlights

- Enabling cryo-preparation of (nano)particles for the atom probe.
- Characterization of surface and bulk elemental distribution of GaPt model SCALMS.

KEYWORDS
atom probe tomography, catalyst particles, cryo preparation, nanoparticles

1 | INTRODUCTION

The characterization of catalyst particles in terms of chemical composition and chemical distribution is of high interest to understand the catalyst behavior. To reveal this information, atom probe tomography (APT) is a suitable measurement method, as it exhibits chemical sensitivity and a near atomic scale spatial resolution. (Felfer et al., 2014; Frierdich et al., 2019; Heck et al., 2014; Josten & Felfer, 2021; Kim et al., 2020; Kim, Antonov et al., 2022; Kim, Yoo et al., 2022; Li et al., 2014; Mosiman et al., 2021; Tedsree et al., 2011; Xiang et al., 2022; Yu et al., 2012).

Even though literature suggests various approaches to measure (nano)particles in the APT (Felfer et al., 2015; Josten & Felfer, 2021; Kim et al., 2018; Li et al., 2014; Miller & Russell, 2007), no broadly applicable strategy for the fabrication of specimens from (nano)particles exists. Commonly, the tip lacks mechanical stability, thus reducing the measurement output, due to fracture events (Heck et al., 2014; Kim et al., 2018; Mosiman et al., 2021).

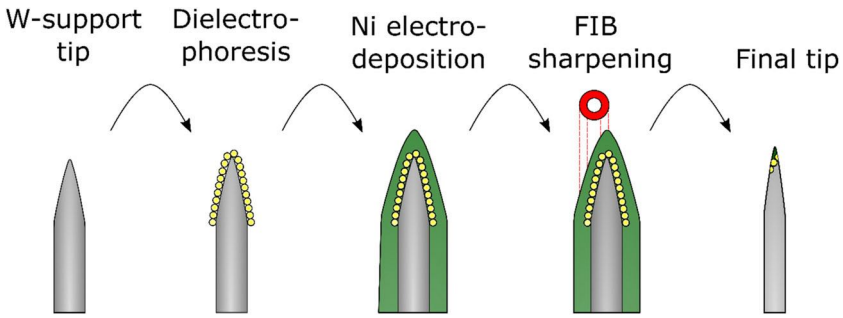

FIGURE 1 Schematic display of the nanoparticle (NP) preparation approach presented in this paper. The particles are applied to a tungsten (W) support tip via dielectrophoresis (DEP). This compound is encapsulated in nickel (Ni) via electrodeposition (ED): By FIB fine milling, the atom probe tomography (APT) tip is sharpened.

In general, nanoparticle (NP) preparation approaches can be divided into three different kinds (Felfer et al., 2015): *(a)* direct measurement after application of NPs on a support tip via (di)electrophoresis ((D)EP), *(b)* coating of particles on a flat support with subsequent Focused Ion Beam (FIB) lift-out, and *(c)* an agglomerate lift-out followed by fine milling.

Further direct application methods, related to the *(a)* (D)EP approach, include a pick-method from a TEM grid (Josten & Felfer, 2021), the manipulation of particles with a micromanipulator (Miller & Russell, 2007), and drop-coating onto pre-sharpened silicon microtips (Heck, 2017; Heck et al., 2014). In these approaches, the particles are subsequently coated.

The more common approach is the application of particles onto a flat substrate *(b)*, followed by a coating procedure. For the encapsulation, deposition techniques like atomic layer deposition (Frierdich et al., 2019; Heck et al., 2014; Larson et al., 2015; Mosiman et al., 2021), electrodeposition (ED) (D. Kim et al., 2017; Kim, Antonov, et al., 2022; Kim et al., 2018; Kim, Yoo, et al., 2022; Xiang et al., 2022), and sputter coating (Adineh et al., 2017; Felfer et al., 2014, 2015; Mosiman et al., 2021) are used. To achieve a tip geometry, a lift-out is performed on this compound. This has the downside that the lift-out adds considerable preparation time and additional potential points of failure, like the weld that is needed to fasten the lift-out to the support tip.

In this paper, we introduce a workflow that allowed us to produce stable APT specimens from gallium (Ga) particles in suspension. The workflow enables a swift and simple specimen preparation without the need of a lift-out procedure and allows cryo-preparation with minimum effort. We achieved this, by combining DEP and Ni-ED in a suitable way.

Both methods (EP and ED) were already described in literature in relation with APT. EP was used by (Li et al., 2014; Tedsree et al., 2011; Yu et al., 2012) to prepare small NPs, with a diameter below 10 nm, directly on a support tip. Here, field evaporation effects impede sensible interpretation of the APT results. On the other side, ED was used in various papers with successfully performed APT experiments (El-Zoka et al., 2017; Kim et al., 2017; Kim et al., 2020; Kim, Antonov, et al., 2022; Kim et al., 2018; Kim, Yoo, et al., 2022; Mouton et al., 2017; Xiang et al., 2022). Despite of being used to fill porous structures (El-Zoka et al., 2017; Mouton et al., 2017), also nanostructures (Kim et al., 2020; Kim, Yoo, et al., 2022) and nanoparticles (Kim et al., 2017; Kim, Antonov, et al., 2022; Kim et al., 2018; Xiang et al., 2022) were successfully measured. Here, the coating was performed onto a flat surface, where the particles were dispersed. A subsequent FIB lift-out procedure enables the measurement of particles with APT.

An overview of the combined DEP- and ED-approach is shown in Figure 1. In a first step, the particles are directly applied to a tungsten (W) support tip via DEP. In a second step, the particles are encapsulated with Ni-ED. To achieve a suitable geometry for the atom probe, this compound is fine-milled in the FIB to form an APT tip. The advantage of this workflow includes the swift preparation, which avoids a time consuming FIB lift-out. It also allows for a simple adaptation to fine-milling at cryo-temperatures in current cryo-setups. This method also does not rely on much additional equipment besides a FIB, which is available in many APT labs.

The introduced workflow is deployed on a catalyst system with low melting temperature. The so called *Supported Catalytically Active Liquid Metal Solutions* (SCALMS) is a novel catalyst type that enables single-atom catalysis at dynamic gas-alloy interfaces (Bauer et al., 2019; Raman et al., 2019, 2021; Taccardi et al., 2017). Typically, low melting materials, like Ga, are doped with a low amount of catalytic active metal. The catalyst is employed in dehydrogenation reactions (Raman et al., 2021; Taccardi et al., 2017). We believe this method is applicable at least to other metallic, potentially also non-metallic inorganic particles in dispersion, since nothing in the preparation approach is specific to the particle type. In the following paragraphs, our workflow is demonstrated based on the investigation of SCALMS particles.

2 | INSTRUMENTATION

The preparation of the investigated GaPt-SCALMS system is described in detail in (Raman et al., 2021). Ga is ultrasonicated in isopropanol for 30 min, until it forms Ga-droplets. Platinum (Pt) is added via galvanic displacement. For this, H_2PtCl_6 is added to the solution and mixed gently for 30 min. As a last step, the powder is washed with ethanol, before it is dried overnight. For the investigation with the atom probe, the particles were prepared without a porous support. The Pt content was adjusted to 2 at%. The Ni-electrolyte was prepared by mixing 200 g H_20, 60 g $Ni(SO_3NH_2)_2$ and 9 g of H_3BO_3. For the APT support tip, W-wire is clamped into a copper-tube for simple manageability of the tip. The W-wire is then etched in 5%

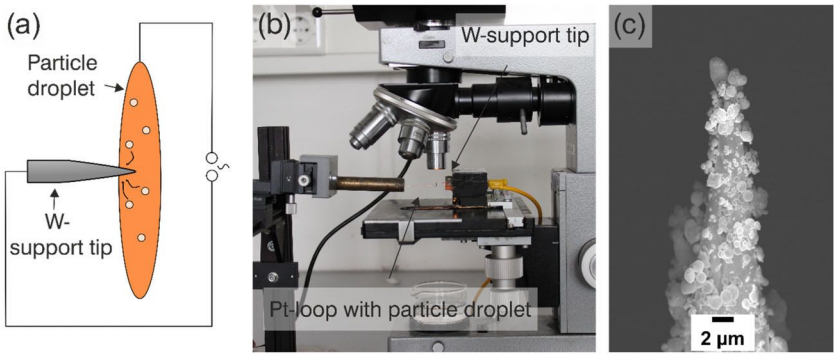

FIGURE 2 (a) shows the schematic process behind the particle application via DEP. The practical setup is displayed in (b). A droplet with the particle suspension is inserted into a Platinum (Pt) loop, while the W-tip is immerged in the droplet without contacting the Pt-loop. The microscope ensures, that the tip apex is dipped into the droplet. By applying an AC voltage between the W-support tip and the Pt-loop containing the droplet, the particles move towards the tip. (c) shows a typical tip after the DEP, where a current of 8 V was applied for 20 s.

sodium hydroxide (NaOH) aqueous solution (Gault et al., 2012; Tsong, 1990). The applied voltage was 5 V. The tips were rinsed with distilled water and 99.9% isopropyl (Nanoprotect GmbH, Germany). Scanning electron microscopy (SEM) and focused ion beam (FIB) milling were performed with an XB540 FIB-SEM (Carl Zeiss Microscopy, Germany). The plasma cleaning was carried out inside the FIB-SEM with a built-in device (XEI Scientific Inc., USA), using nitrogen to create the plasma. Imaging was done with an electron beam accelerating voltage of 3 kV and beam current of 2 nA. The selected FIB currents and acceleration voltages are described in detail in the following paragraph. Preparation at cryogenic-temperatures was performed with a cryo-stage (Quorum Technologies Limited, United Kingdom). A temperature of −160°C was maintained during the experiments. Transmission electron microscopy (TEM) was performed at an FEI Titan Themis^3 300 double-aberration-corrected instrument (Thermo Fisher Scientific, USA). The tips were analyzed using correlative STEM-EDXS measurements. The images were acquired at 300 keV with 30 µs dwell-time and a pixel-size of 1.53 nm. Spectrum image quantification was optimized with the help of *Thermo Scientific Velox* Software (3.8.1.14) using pre-filtering of 1.0 gaussian blur, 100 nm sample thickness absorption correction, and Schreiber-Wims Ionization cross-section model.

The APT measurements were carried out in a CAMECA LEAP 4000X HR (CAMECA, France) using laser assisted field evaporation. During the measurements, the specimen base temperature was 50 K, the pulse energy 50 pJ, and the pulse repetition rate 125 kHz. Reconstruction and interpretation were done using CAMECA IVAS 3.6.8 (CAMECA, France) and MATLAB (MathWorks, United States of America) scripts that were developed in-house and are accessible via Github (https://github.com/peterfelfer/Atom-Probe-Toolbox).

3 | METHODS: DESCRIPTION OF THE DEVELOPED WORKFLOW

In the first step of the workflow, the particles are attached to a W-support tip via DEP (see Figure 1). We chose W as support tip material, as it is easy to electropolish, robust, and therefore a commonly used tip material in APT (Miller & Russell, 2007).

DEP is the effect of the movement of particles in an inhomogeneous electric field (Pohl, 1951). By exposing particles in a dielectric medium to a homogenous electric field, a dipole moment is induced into the particles. The induced charges are of equal magnitude on two sides of the particles. In case of an inhomogeneous field, the charge on one side of the particles is smaller, which leads to the motion of the particles. Detailed description of DEP, including influence factors like frequency and medium permittivity, can be found in various publications, reviews, and books (Boote & Evans, 2005; Jones, 1995; Liu & Bau, 2004; Pesch & Du, 2021; Pethig, 2017; Pohl, 1951; Pohl et al., 1978). We exploit this induced particle movement to attach the particles in solution to the support tip. The basic setup we use is shown in Figure 2a. In our case, the GaPt-SCALMS particles are dispersed in isopropyl alcohol. One droplet is inserted into a Pt-wire loop, the apex of the W-support tip is dipped into the droplet. The employed setup is similar to commonly used electropolishing setups in APT (see Figure 2b). After applying an AC voltage of 8 V for 20 s, the GaPt particles stick to the W-tip. An exemplary tip is displayed in Figure 2c. By varying voltage and time, the number of attached particles can be adapted. The suitable voltage and time were found via trial and error. It is desirable to get a homogenous coverage, as this simplifies the FIB-milling step and increases the chance to incorporate a particle into the final tip.

As indicated in Figure 1, the second step of the workflow consists of the encapsulation of the particle-tip compound. This is achieved by electrodepositing Ni (see Figure 3a,b). In the following, the theory behind the ED-process is described shortly. It will be explicitly concentrated on the points that are of interest for the coating of APT tips, and the practical aspects of the deposition will be discussed. For further information, the reader is referred to literature, that describes the electroplating process in detail (Giurlani et al., 2018; Hanson & Hanson, 2019; Kanani, 2006; Paunovic & Schlesinger, 2006; Schlesinger & Paunovic, 2010).

Concerning the preparation of a bulk work piece, in-line plating processes require several cleaning steps before the ED-process (Kanani, 2006). Transferred to the tip preparation, thoroughly cleaning of the W-tip with distilled water and clean isopropyl, preceding to the DEP-step proved to be important. If the tip is investigated in the SEM after DEP to validate the distribution and appearance of the deposited particles, plasma cleaning is particularly important to remove any carbon residue deposited by the electron beam. Figure 3c shows the adhesion of an ED Ni-layer intentionally contaminated with carbon by the electron beam on one side. Even if no electron imaging takes

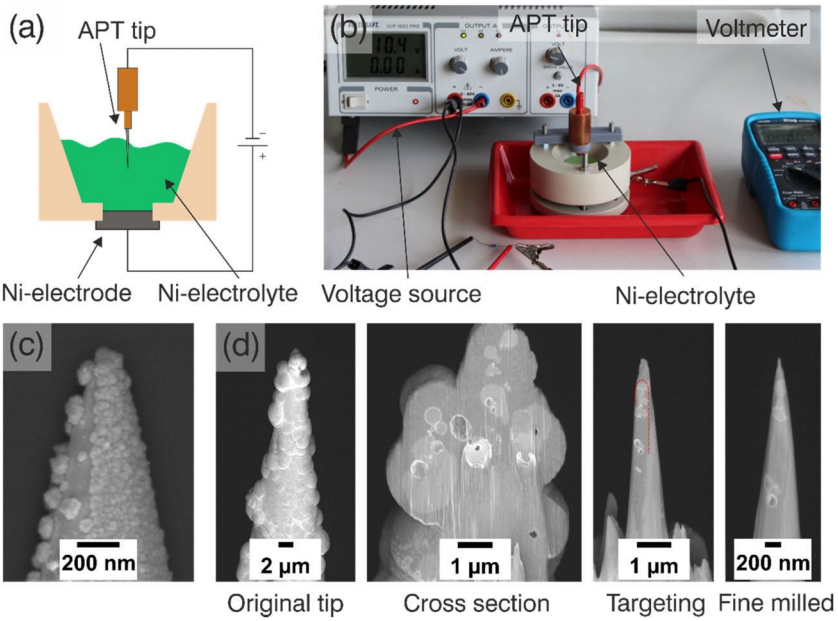

FIGURE 3 (a) shows a scheme for electrodepositing Ni on the tip, (b) displays the ED setup. The tip is dipped into the Ni-electrolyte, the electrode is positioned in the opposite location. The voltage is applied with the voltage source and verified by the voltmeter. In (c) the tip was imaged in the SEM prior to the Ni deposition. It can be clearly distinguished between the imaged area (left side of tip), where the adsorbents of the electron beam worsen the coating adhesion, and the pristine part of the tip. Here, the coating is stable and dense. (d) displays the steps to fine-mill the APT tip. In the first step, a cross section is cut to make the particles visible. A chosen particle is centered in the tip. In a last step, the tip is thinned to a suitable diameter and shortened (indicated by the red dotted line), so the particle is incorporated near the tip apex.

place, it is advisable to perform plasma cleaning prior to further processing, to clean possible carbon contaminants from the particle. In general, plasma cleaning helps to remove carbon-adsorbents from the tip and improves the adherence of the coating.

The principle of the deposition process is depicted in Figure 3a, the setup we use for the ED is shown in Figure 3b. The anode at the bottom of the electrolyte vat and the cathodically polarized specimen inserted from the top are in contact with the Ni-electrolyte. After applying a DC current, the Ni-cations electrode posit on the negatively charged cathode (Hanson & Hanson, 2019; Kanani, 2006). Apart from the Ni-anode in our setup, another typical electrode material, employable for various electrolytes, is platinum (Kanani, 2006). For the Ni-deposition, current properties are set to 10 V and 1 mA. A typical result for a Ni-coated tip after 40 s deposition is shown in Figure 3d. The Ni coating is dense and shows no cracks or delaminations.

There are several practical advantages in coating solely the tip apex, compared to the coating of a flat bulk specimen, or a whole APT tip. The small sample surface enables short deposition times. With coating times around 40 s per tip, a high specimen throughput is possible. Additionally, the endurance time of the electrolyte is increased in direct comparison of the deposition on a bulk sample, as the small deposition volume reduces Ni-depletion in the electrolyte. The sole insertion of the top of the APT tips, leads to a defined coating environment. Inserting the whole tip (particles, W-wire, and copper tube, which is holding the wire) complicates the electrochemical environment. Copper dissolves into the electrolyte, and consequently copper, instead of Ni, deposits on the tip (see Figure 1SI). Also, deposition times are increased due to the increased specimen surface. Figure 2SI displays the variation in the coating thickness, depending on the coated volume, while applying the same coating parameters.

The most important advantage is the geometry of the resulting specimen. The tip can be directly FIB-milled, without the extra step of a FIB lift-out. The consumed time for the preparation itself is drastically reduced, and the avoidance of a Pt-weld improves the tip stability. The milling strategy is displayed in Figure 3d. The components of the tip (Ni-Matrix, particles, and W-wire) are distinguishable during the FIB preparation. By cutting a cross section, the operator can target a specific particle and prepare the particle to be inside of the APT tip. For the case of smaller particles, which are not as visible as in Figure 3d, the operator can target the W-Ni interface, where the particles are located.

Since the volume to be removed is small, FIB beam currents of 250 pA at 10 kV are sufficient for the first milling step, which is the cross-section. For the targeting of specific particles and the finer milling steps, 10 and 5 kV FIB beam voltages are appropriate. As a last step, shortening of the tip with low beam voltages of 5 and 2 kV enables the positioning of the particles in the tip with a small distance to the tip apex. Using low voltages and currents reduces Ga implantation. Additionally, it enables the FIB operator to confirm that the Ni-coating is not destroyed by the FIB beam and the particle surface is still intact.

What needs to be highlighted in the cross section is a possible influence of the FIB beam on the particles. In Figure 3d voids inside of particles can be observed in the case of Ga particles. The FIB beam is known for increasing the local temperature (Ishitani & Kaga, 1995; Shukla et al., 2009) and for introducing defects into low melting materials (Dantas de Morais et al., 2014). As the melting point of pure Ga is at 29.7°C (Meyers, 2001), the voids visible in the cross-section of Figure 3d likely arise from an interaction of the FIB beam with the particles.

For the reduction of the FIB beam influence on the sample, the specimen temperature was decreased to −160°C during FIB milling. Our near-tip-shape preparation and lift-out free workflow enables the potential to directly insert the samples into a cryo-stage to avoid a cryo lift-out. Even though progresses in the area of cryo lift-outs of TEM lamellas are reported in literature (Kuba et al., 2021; Parmenter & Nizamudeen, 2021; Schaffer et al., 2019), cryo lift-outs

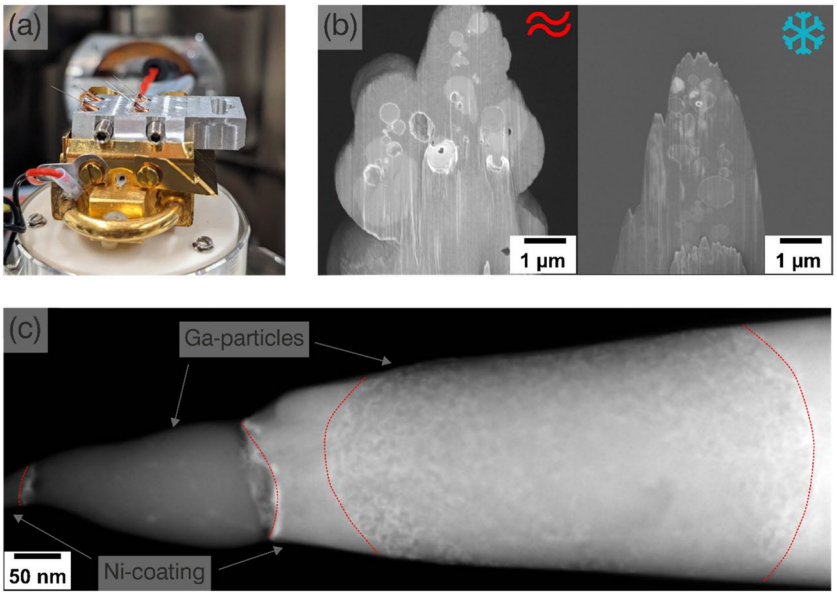

FIGURE 4 (a) shows the employed cryo-stage and custom-made holder. The pre-tilt holder enables direct FIB milling and avoids the need of extensive stage movement. (b) displays the direct comparison between a cross-section of embedded GaPt particles, done at room- and cryo-temperatures. At room temperature, a distinct influence of the FIB beam can be observed. This is manifested by the "pores" that are not visible in the cross-section at cryo-temperatures. In (c) the STEM measurement of a tip prepared at cryo-temperatures illustrates two incorporated particles, which are separated by the Ni-matrix. The particles' interfaces are highlighted by the red dotted lines. A Ni-cap on the tip apex is still intact and protects the particle surface. A STEM EDXS investigation of this tip is shown in Figure 6SI.

for APT specimens are still not established. There are few reports described in the literature (Chen et al., 2021; Schreiber et al., 2018), and often expensive hardware is needed (Perea, 2020). By avoiding this preparation step, we enable the preparation of particles for APT without an established cryo lift-out procedure. Figure 4a shows the deployed setup for the cryo-preparation. A special holder we developed (see Figure 4a) enables the preparation of multiple tips without the need to exchange samples. A direct comparison between a cross section done at room-temperature and at cryo-temperature is displayed in Figure 4b. The absence of pores at cryo-temperature indicates a reduced FIB beam influence. Figure 4c shows a STEM image of a cryo-prepared atom probe tip. The particles are clearly distinguishable from the Ni-coating material. The Ni-capping is still intact and thus the surface of the particle is not cut.

4 | RESULTS AND DISCUSSION

4.1 | APT tips prepared at room temperature

The tips prepared at room temperature run in a stable way in the atom probe. No major fracture events occurred, as neither voltage jumps, nor distinctly increased detection rates were observed (see Figure 3SI). So it can be assumed that no particle parts got lost due to fracture events and that the atoms of the reconstructed volumes were field evaporated in sequence.

The 3D reconstructions of the room-temperature prepared specimens are shown in Figure 5a. In both specimens, the surface of the nanoparticle was captured, evident by the transition to the encapsulating Ni.

Both measured volumes show two chemical distinct areas. Those regions are indicated by the orange and blue isosurfaces in Figure 5a. The orange isosurfaces mark a region that is rich in Ga and O atoms. Ga is known for forming an oxide layer, when exposed to air (Regan et al., 1997; Wang et al., 2021), so the measurement of the O-rich region is coinciding with the formation of an oxide layer. The blue isosurfaces represent a Pt-rich region. In average, the Ga concentration in the regions is at 9.1 at%. This fits to the Ga solubility in Pt, which amounts to 6 at% at room temperature according to Guex et al. (Guex & Feschotte, 1976). The concentration evolution on the Ga-oxide-Pt-interface is shown in Figure 5b. The transition between the Ga-oxide and the Pt-rich area is clearly pronounced. The preparation of Ga particles with a Ga-FIB may lead to ion implantation and may thus influence the interpretation of the interaction between Ga and Pt. To exclude this, we analyzed the Ga content inside of the Ni-capping (see Figure 4SI) and found a minor Ga content. The concentration evolution in Figure 5b also underlines a negligible Ga FIB-influence, as the interface between Pt- and Ga-rich regions is pronounced distinctly.

4.2 | APT tips prepared at cryo temperatures

The mass spectrum of a cryo-prepared tip is displayed in Figure 5c. The Ga-peaks at 69 and 71 Da are distinctly present. Interestingly, the measured mass spectrum mainly consists of Ga, without numerous other peaks. To highlight the absence of Pt, the theoretical location of Pt-peaks is indicated with red squares. The observed O-atoms are mainly present in the Ni-capping (see Figure 5SI), proving that the particle area measured during this experiment, consisted of pure Ga. The Ga is neither oxidized, nor any measurable amount of Pt is dissolved. In direct comparison to the room-temperature prepared tip, we assume that the interface between the oxide and the matrix is not stable and fractured during the cryo-experiment. To underline this assumption, the voltage curve and the detection rate plot of the cryo measurement are shown in Figure 5SI. The measurement of the first particle atoms is accompanied by an increased detection rate, indicating a fracture event at the oxide–matrix interface. The further-on measured volume solely comprises the Ga-matrix. The fracture does not limit the applicability of the presented workflow, as the fracture

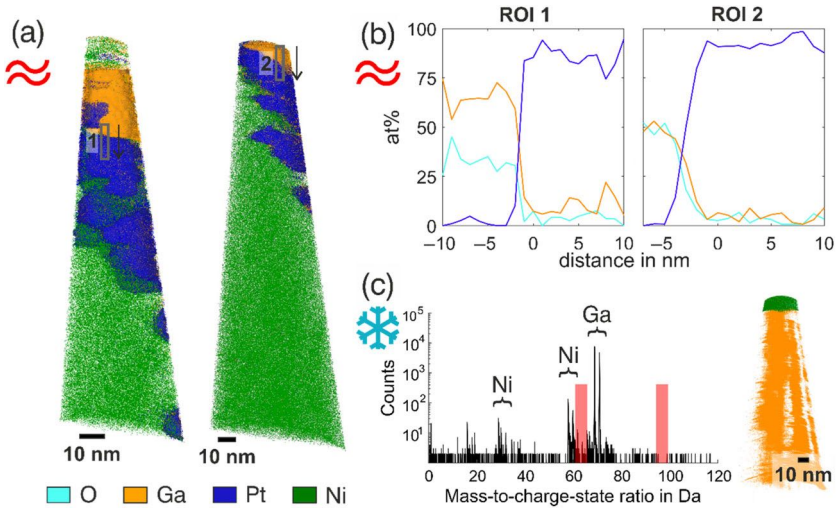

FIGURE 5 (a) displays the reconstructions of the room-temperature prepared tips. The blue isosurface represents a Pt-rich region, while the orange isosurface assigns the Ga-oxide. The squares represent the regions of the ROIs that are used for further concentration evolution analysis in (b). (b) shows the concentration evolution of Ga, Pt and O between the Ga- and Pt-rich region on the basis of 2 × 2 nm ROIs. The Ga-rich region also shows an enrichment of O, thus implying the formation of a Ga-oxide layer. (c) displays the mass spectrum and the reconstruction of the cryo-prepared tip. The red squares in the mass spectrum highlight the region, where Pt would be found. The measured volume consists mainly of pure Ga, the central peaks in the mass spectrum. The location of the Ni-peaks is marked with the according brackets. The reconstruction shows the Ni-capping and consecutively the Ga-matrix. While the Ni-capping evaporated evenly, the Ga-matrix evaporated in a patchy-way. The evaporation seems to be characteristic for Ga and is not an effect of the preparation method.

arises from an unstable interface inside of the particle, which is not in the area of influence of the instrument handler.

By combining the findings of the APT measurements at cryo- and at room temperature with STEM images, we are able to draw a precise picture of the particles chemistry. STEM EDS measurements in Figure 6SI show a higher Pt content in the particle shell and a high Ga-concentration inside of the particle. On the basis of our cryo-APT measurement, where we measured the particle matrix, we conclude that the interior of the particles consists of pure Ga. In context with the room-temperature APT measurement, where the particle-surface was measured, we see that the surface is enriched with Pt, in which a small amount of Ga is dissolved. Beneath the Pt-rich layer, a Ga-oxide layer exists. It is likely that during the preparation at room temperature, the interior of the particles is removed by effects other than sputtering. This would explain why the room temperature FIB milled specimens usually show the surface region first, while for the cryo FIBed specimens we tend to observe the particle volume. This is, however, rather specific to the low melting point particles used in this study. Coincidentally, this gives a comprehensive image of the GaPt-SCALMS particles: a pure Ga matrix is surrounded by a Ga-oxide/Pt enriched layer.

5 | CONCLUSION

The described preparation workflow enables the preparation of atom probe specimens from particles in dispersion, with reasonable throughput and an experimental setup that is quite accessible for most APT labs. The combination of DEP and ED directly on top of an APT tip produces a near-tip shaped geometry of the sample before the FIB milling steps. Avoiding a FIB lift-out routine saves preparation time and enables a high preparation rate of APT tips. In the case of the Ga particles used in this study, it was also possible to easily position the particles at the tip apex. This ability may vary based on particle material and size. Without the use of lift-outs and following a routine that does not demand stage rotations, we could also employ cryo-milling with a cryo-stage. This was a requirement for the successful preparation of the particle interiors of the low-melting point particles in this study.

This workflow enabled us to investigate the atomic structure of SCALMS particles. We showed the interface of SCALMS particles to consist of a Ga-oxide and a pure Pt layer after the galvanic displacement. Via cryo-FIB the existence of a pure Ga matrix was discovered. The APT investigations revealed, that the Ga-oxide layer may act as a barrier for the Pt, as it is not dissolved inside of the Ga matrix.

AUTHOR CONTRIBUTIONS

Nora Vorlaufer: Investigation; writing – original draft; methodology; visualization; writing – review and editing; formal analysis; conceptualization. **Jan Josten:** Investigation; methodology; writing – review and editing. **Simon Carl:** Investigation; writing – review and editing. **Erik Göbel:** Investigation. **Alexander Søgaard:** Writing – review and editing; methodology. **Nicola Taccardi:** Writing – review and editing; methodology. **Erdmann Spiecker:** Writing – review and editing; supervision; funding acquisition. **Peter Felfer:** Writing – review and editing; conceptualization; funding acquisition; supervision.

ACKNOWLEDGMENTS

The authors gratefully acknowledge financial support by the DFG through the SFB 1452 CLINT (Project 431791331) and the research training group GRK 1896 "*In Situ* Microscopy with Electrons, X-rays and Scanning Probes." Open Access funding enabled and organized by Projekt DEAL.

CONFLICT OF INTEREST STATEMENT

The authors declare none.

DATA AVAILABILITY STATEMENT

The data that support the findings of this study are available from the corresponding author upon reasonable request.

ORCID

Nora Vorlaufer https://orcid.org/0009-0004-4305-3951

REFERENCES

Adineh, V. R., Marceau, R. K. W., Chen, Y., Si, K. J., Velkov, T., Cheng, W., Li, J., & Fu, J. (2017). Pulsed-voltage atom probe tomography of low conductivity and insulator materials by application of ultrathin metallic coating on nanoscale specimen geometry. *Ultramicroscopy*, *181*, 150–159. https://doi.org/10.1016/j.ultramic.2017.05.002

Bauer, T., Maisel, S., Blaumeiser, D., Vecchietti, J., Taccardi, N., Wasserscheid, P., Bonivardi, A., Görling, A., & Libuda, J. (2019). Operando DRIFTS and DFT study of propane dehydrogenation over solid- and liquid-supported Ga $_x$ Pt $_y$ catalysts. *ACS Catalysis*, *9*(4), 2842–2853. https://doi.org/10.1021/acscatal.8b04578

Boote, J. J., & Evans, S. D. (2005). Dielectrophoretic manipulation and electrical characterization of gold nanowires. *Nanotechnology*, *16*(9), 1500–1505. https://doi.org/10.1088/0957-4484/16/9/015

Chen, Y.-S., Griffith, M. J., & Cairney, J. M. (2021). Cryo atom probe: Freezing atoms in place for 3D mapping. *Nano Today*, *37*, 101107. https://doi.org/10.1016/j.nantod.2021.101107

Dantas de Morais, L., Chevalliez, S., & Mouleres, S. (2014). Low temperature FIB cross section: Application to indium micro bumps. *Microelectronics Reliability*, *54*(9–10), 1802–1805. https://doi.org/10.1016/j.microrel.2014.08.004

El-Zoka, A. A., Langelier, B., Botton, G. A., & Newman, R. C. (2017). Enhanced analysis of nanoporous gold by atom probe tomography. *Materials Characterization*, *128*, 269–277. https://doi.org/10.1016/j.matchar.2017.03.013

Felfer, P., Benndorf, P., Masters, A., Maschmeyer, T., & Cairney, J. M. (2014). Revealing the distribution of the atoms within individual bimetallic catalyst nanoparticles. *Angewandte Chemie International Edition*, *53*(42), 11190–11193. https://doi.org/10.1002/anie.201405043

Felfer, P., Li, T., Eder, K., Galinski, H., Magyar, A. P., Bell, D. C., Smith, G. D. W., Kruse, N., Ringer, S. P., & Cairney, J. M. (2015). New approaches to nanoparticle sample fabrication for atom probe tomography. *Ultramicroscopy*, *159*, 413–419. https://doi.org/10.1016/j.ultramic.2015.04.014

Frierdich, A. J., Saxey, D. W., Adineh, V. R., Fougerouse, D., Reddy, S. M., Rickard, W. D. A., Sadek, A. Z., & Southall, S. C. (2019). Direct observation of nanoparticulate goethite recrystallization by atom probe analysis of isotopic tracers. *Environmental Science & Technology*, *53*(22), 13126–13135. https://doi.org/10.1021/acs.est.9b04191

Gault, B., Moody, M. P., Cairney, J. M., & Ringer, S. P. (2012). *Atom probe microscopy* (Vol. 160). Springer. https://doi.org/10.1007/978-1-4614-3436-8

Giurlani, W., Zangari, G., Gambinossi, F., Passaponti, M., Salvietti, E., Di Benedetto, F., Caporali, S., & Innocenti, M. (2018). Electroplating for decorative applications: Recent trends in research and development. *Coatings*, *8*(8), 260. https://doi.org/10.3390/coatings8080260

Guex, P., & Feschotte, P. (1976). Les systèmes binaires platine-aluminium, platinegallium et platine-indium. *Journal of the Less Common Metals*, *46*(1), 101–116. https://doi.org/10.1016/0022-5088(76)90183-1

Hanson, D., & Hanson, D. (2019). *Electroplating*. The Crowood Press.

Heck, P. R. (2017). The enigmatic origin of meteoritic nanodiamonds—An approach with atom-probe tomography. *Microscopy and Microanalysis*, *23*(S1), 2276–2277. https://doi.org/10.1017/S1431927617012041

Heck, P. R., Stadermann, F. J., Isheim, D., Auciello, O., Daulton, T. L., Davis, A. M., Elam, J. W., Floss, C., Hiller, J., Larson, D. J., Lewis, J. B., Mane, A., Pellin, M. J., Savina, M. R., Seidman, D. N., & Stephan, T. (2014). Atom-probe analyses of nanodiamonds from Allende. *Meteoritics & Planetary Science*, *49*(3), 453–467. https://doi.org/10.1111/maps.12265

Ishitani, T., & Kaga, H. (1995). Calculation of local temperature rise in focused-ion-beam sample preparation. *Journal of Electron Microscopy*, *44*(5), 331–336. https://doi.org/10.1093/oxfordjournals.jmicro.a051185

Jones, T. B. (1995). *Electromechanics of particles* (1st ed.). Cambridge University Press. https://doi.org/10.1017/CBO9780511574498

Josten, J. P., & Felfer, P. J. (2021). Atom probe analysis of nanoparticles through pick and coat sample preparation. *Microscopy and Microanalysis*, *28*(4), 1188–1197. https://doi.org/10.1017/S1431927621000465

Kanani, N. (2006). *Electroplating: Basic principles, processes and practice* (1st ed.). Elsevier Science.

Kim, D., Kley, C. S., Li, Y., & Yang, P. (2017). Copper nanoparticle ensembles for selective electroreduction of CO $_2$ to C $_2$ –C $_3$ products. *Proceedings of the National Academy of Sciences of the United States of America*, *114*(40), 10560–10565. https://doi.org/10.1073/pnas.1711493114

Kim, S., Lim, J., Sahu, R., Kasian, O., Stephenson, L. T., Scheu, C., & Gault, B. (2020). Direct imaging of dopant and impurity distributions in 2D MoS_2. *Advanced Materials*, *32*(8), 1907235. https://doi.org/10.1002/adma.201907235

Kim, S.-H., Antonov, S., Zhou, X., Stephenson, L. T., Jung, C., El-Zoka, A. A., Schreiber, D. K., Conroy, M., & Gault, B. (2022). Atom probe analysis of electrode materials for Li-ion batteries: Challenges and ways forward. *Journal of Materials Chemistry A*, *10*(9), 4926–4935. https://doi.org/10.1039/D1TA10050E

Kim, S.-H., Kang, P. W., Park, O. O., Seol, J.-B., Ahn, J.-P., Lee, J. Y., & Choi, P.-P. (2018). A new method for mapping the three-dimensional atomic distribution within nanoparticles by atom probe tomography (APT). *Ultramicroscopy*, *190*, 30–38. https://doi.org/10.1016/j.ultramic.2018.04.005

Kim, S.-H., Yoo, S.-H., Chakraborty, P., Jeong, J., Lim, J., El-Zoka, A. A., Zhou, X., Stephenson, L. T., Hickel, T., Neugebauer, J., Scheu, C., Todorova, M., & Gault, B. (2022). Understanding alkali contamination in colloidal nanomaterials to unlock grain boundary impurity engineering. *Journal of the American Chemical Society*, *144*(2), 987–994. https://doi.org/10.1021/jacs.1c11680

Kuba, J., Mitchels, J., Hovorka, M., Erdmann, P., Berka, L., Kirmse, R., König, J., De Bock, J., Goetze, B., & Rigort, A. (2021). Advanced cryo-tomography workflow developments – Correlative microscopy, milling automation and cryo-lift-out. *Journal of Microscopy*, *281*(2), 112–124. https://doi.org/10.1111/jmi.12939

Larson, D. J., Giddings, A. D., Wu, Y., Verheijen, M. A., Prosa, T. J., Roozeboom, F., Rice, K. P., Kessels, W. M. M., Geiser, B. P., & Kelly, T. F. (2015). Encapsulation method for atom probe tomography analysis of nanoparticles. *Ultramicroscopy*, *159*, 420–426. https://doi.org/10.1016/j.ultramic.2015.02.014

Li, T., Bagot, P. A. J., Christian, E., Theobald, B. R. C., Sharman, J. D. B., Ozkaya, D., Moody, M. P., Tsang, S. C. E., & Smith, G. D. W. (2014). Atomic imaging of carbon-supported Pt, Pt/Co, and Ir@Pt

Nanocatalysts by atom-probe tomography. *ACS Catalysis*, *4*(2), 695–702. https://doi.org/10.1021/cs401117e

Liu, H., & Bau, H. H. (2004). The dielectrophoresis of cylindrical and spherical particles submerged in shells and in semi-infinite media. *Physics of Fluids*, *16*(5), 1217–1228. https://doi.org/10.1063/1.1649237

Meyers, R. A. (Ed.). (2001). *Encyclopedia of physical science and technology* (3rd ed.). Elsevier Science.

Miller, M. K., & Russell, K. F. (2007). Atom probe specimen preparation with a dual beam SEM/FIB miller. *Ultramicroscopy*, *107*(9), 761–766. https://doi.org/10.1016/j.ultramic.2007.02.023

Mosiman, D. S., Chen, Y., Yang, L., Hawkett, B., Ringer, S. P., Mariñas, B. J., & Cairney, J. M. (2021). Atom probe tomography of encapsulated hydroxyapatite nanoparticles. *Small Methods*, *5*(2), 2000692. https://doi.org/10.1002/smtd.202000692

Mouton, I., Printemps, T., Grenier, A., Gambacorti, N., Pinna, E., Tiddia, M., Vacca, A., & Mula, G. (2017). Toward an accurate quantification in atom probe tomography reconstruction by correlative electron tomography approach on nanoporous materials. *Ultramicroscopy*, *182*, 112–117. https://doi.org/10.1016/j.ultramic.2017.06.007

Parmenter, C. D., & Nizamudeen, Z. A. (2021). Cryo-FIB-lift-out: Practically impossible to practical reality. *Journal of Microscopy*, *281*(2), 157–174. https://doi.org/10.1111/jmi.12953

Paunovic, M., & Schlesinger, M. (2006). *Fundamentals of electrochemical deposition* (2nd ed.). John Wiley & Sons.

Perea, D. (2020). Advanced Cryo-FIB specimen preparation and handling of environmentally sensitive materials for APT analysis. *Microscopy and Microanalysis*, *26*(S2), 2094–2095. https://doi.org/10.1017/S1431927620020425

Pesch, G. R., & Du, F. (2021). A review of dielectrophoretic separation and classification of non-biological particles. *Electrophoresis*, *42*(1–2), 134–152. https://doi.org/10.1002/elps.202000137

Pethig, R. (2017). *Dielectrophoresis: Theory, methodology, and biological applications*. John Wiley & Sons, Inc.

Pohl, H. A. (1951). The motion and precipitation of suspensoids in divergent electric fields. *Journal of Applied Physics*, *22*(7), 869–871. https://doi.org/10.1063/1.1700065

Pohl, H. A., Pollock, K., & Crane, J. S. (1978). Dielectrophoretic force: A comparison of theory and experiment. *Journal of Biological Physics*, *6*(3–4), 133–160. https://doi.org/10.1007/BF02328936

Raman, N., Maisel, S., Grabau, M., Taccardi, N., Debuschewitz, J., Wolf, M., Wittkämper, H., Bauer, T., Wu, M., Haumann, M., Papp, C., Görling, A., Spiecker, E., Libuda, J., Steinrück, H.-P., & Wasserscheid, P. (2019). Highly effective propane dehydrogenation using Ga–Rh supported catalytically active liquid metal solutions. *ACS Catalysis*, *9*(10), 9499–9507. https://doi.org/10.1021/acscatal.9b02459

Raman, N., Wolf, M., Heller, M., Heene-Würl, N., Taccardi, N., Haumann, M., Felfer, P., & Wasserscheid, P. (2021). GaPt supported catalytically active liquid metal solution catalysis for propane dehydrogenation–support influence and coking studies. *ACS Catalysis*, *11*(21), 13423–13433. https://doi.org/10.1021/acscatal.1c01924

Regan, M. J., Tostmann, H., Pershan, P. S., Magnussen, O. M., DiMasi, E., Ocko, B. M., & Deutsch, M. (1997). X-ray study of the oxidation of liquid-gallium surfaces. *Physical Review B*, *55*(16), 10786–10790. https://doi.org/10.1103/PhysRevB.55.10786

Schaffer, M., Pfeffer, S., Mahamid, J., Kleindiek, S., Laugks, T., Albert, S., Engel, B. D., Rummel, A., Smith, A. J., Baumeister, W., & Plitzko, J. M. (2019). A cryo-FIB lift-out technique enables molecular-resolution cryo-ET within native Caenorhabditis elegans tissue. *Nature Methods*, *16*(8), 757–762. https://doi.org/10.1038/s41592-019-0497-5

Schlesinger, M., & Paunovic, M. (Eds.). (2010). *Modern electroplating* (5th ed.). John Wiley & Sons.

Schreiber, D. K., Perea, D. E., Ryan, J. V., Evans, J. E., & Vienna, J. D. (2018). A method for site-specific and cryogenic specimen fabrication of liquid/solid interfaces for atom probe tomography. *Ultramicroscopy*, *194*, 89–99. https://doi.org/10.1016/j.ultramic.2018.07.010

Shukla, N., Tripathi, S. K., Banerjee, A., Ramana, A. S. V., Rajput, N. S., & Kulkarni, V. N. (2009). Study of temperature rise during focused Ga ion beam irradiation using nanothermo-probe. *Applied Surface Science*, *256*(2), 475–479. https://doi.org/10.1016/j.apsusc.2009.07.024

Taccardi, N., Grabau, M., Debuschewitz, J., Distaso, M., Brandl, M., Hock, R., Maier, F., Papp, C., Erhard, J., Neiss, C., Peukert, W., Görling, A., Steinrück, H.-P., & Wasserscheid, P. (2017). Gallium-rich Pd–Ga phases as supported liquid metal catalysts. *Nature Chemistry*, *9*(9), 862–867. https://doi.org/10.1038/nchem.2822

Tedsree, K., Li, T., Jones, S., Chan, C. W. A., Yu, K. M. K., Bagot, P. A. J., Marquis, E. A., Smith, G. D. W., & Tsang, S. C. E. (2011). Hydrogen production from formic acid decomposition at room temperature using a Ag–Pd core–shell nanocatalyst. *Nature Nanotechnology*, *6*(5), 302–307. https://doi.org/10.1038/nnano.2011.42

Tsong, T. T. (1990). *Atom-probe field ion microscopy: Field ion emission, and surfaces and interfaces at atomic resolution*. Cambridge University Press.

Wang, D., Wang, X., & Rao, W. (2021). Precise regulation of Ga-based liquid metal oxidation. *Accounts of Materials Research*, *2*(11), 1093–1103. https://doi.org/10.1021/accountsmr.1c00173

Xiang, W., Yang, N., Li, X., Linnemann, J., Hagemann, U., Ruediger, O., Heidelmann, M., Falk, T., Aramini, M., DeBeer, S., Muhler, M., Tschulik, K., & Li, T. (2022). 3D atomic-scale imaging of mixed Co-Fe spinel oxide nanoparticles during oxygen evolution reaction. *Nature Communications*, *13*(1), 179. https://doi.org/10.1038/s41467-021-27788-2

Yu, K. M. K., Tong, W., West, A., Cheung, K., Li, T., Smith, G., Guo, Y., & Tsang, S. C. E. (2012). Non-syngas direct steam reforming of methanol to hydrogen and carbon dioxide at low temperature. *Nature Communications*, *3*(1), 1230. https://doi.org/10.1038/ncomms2242

SUPPORTING INFORMATION

Additional supporting information can be found online in the Supporting Information section at the end of this article.

How to cite this article: Vorlaufer, N., Josten, J., Carl, S., Göbel, E., Søgaard, A., Taccardi, N., Spiecker, E., & Felfer, P. (2024). Preparation of atom probe tips from (nano)particles in dispersion using (di)electrophoresis and electroplating. *Microscopy Research and Technique*, *87*(3), 476–483. https://doi.org/10.1002/jemt.24448